ARTICLE IN PRESS

Nuclear Inst. and Methods in Physics Research, A ▮ (▮▮▮▮) ▮▮▮–▮▮▮

Contents lists available at ScienceDirect

Nuclear Inst. and Methods in Physics Research, A

journal homepage: www.elsevier.com/locate/nima

Efficient temperature corrections for gamma-ray energy reconstruction in 3-D position-sensitive CdZnTe detectors

Jiawei Xia *, Yuefeng Zhu, Zhong He

2355 Bonisteel Blvd, Ann Arbor, MI 48109, USA

ARTICLE INFO

Keywords:
CdZnTe
Temperature
3-D reconstruction

ABSTRACT

Maintaining good energy resolution in 3-D position-sensitive cadmium zinc telluride (CdZnTe) detectors without temperature regulation is desired in field operations to lower power consumption. This requires several calibration measurements at various ambient temperatures. However, required calibration times and storage space for calibration data increase linearly with working temperature range. In this experiment, gamma-ray interactions were measured by 3-D, position-sensitive CdZnTe detectors read out via VAD_UM v2.2 ASICs at various ambient temperatures. Physical causes of changes in detector behavior were studied. A proposed method to reconstruct events using only one complete calibration measurement, and several faster measurements at different ambient temperatures is discussed. Calibration data estimated using the proposed method showed almost identical performance compared to measured calibration data for measurements for various ambient temperatures at equilibrium. The paper also discusses experimental results that showed good resolution in 3-D CdZnTe detector systems can be achieved even if temperature regulation is fully discarded.

Contents

1. Introduction 1
2. Experimental methods 2
3. Analysis and correction for calibration-temperature drift 3
   3.1. Channel-by-channel gain vs. temperature 3
   3.2. Voxel-by-voxel gain vs. temperature 3
   3.3. Drift time-depth relationship vs. temperature 4
   3.4. Weighting potential crosstalk and nonlinearity vs. temperature 4
   3.5. Performance of temperature-corrected calibration data 4
4. Events reconstruction based on temperature 5
5. Conclusion 6
   Acknowledgments 6
   References 6

1. Introduction

Pixelated, 3-D position-sensitive CdZnTe (3-D CdZnTe) is a promising alternative to High-Purity Germanium (HPGe) detectors. With the state-of-the-art readout technology, the Orion Group at the University of Michigan consistently achieves single-pixel events energy resolutions below 0.40% full-width-at-half-maximum (FWHM) at 661.7 keV for most direct-attachment CdZnTe detectors [1]. In addition to spectroscopy, 3-D position-sensitive CdZnTe detectors have gamma ray and neutron imaging capabilities [2,3]. Furthermore, CdZnTe detectors can be operated at room temperatures, making in-the-field operation of CdZnTe detectors more convenient than HPGe detectors.

However, voxel-by-voxel gain corrections, estimated during calibration, are sensitive to detector temperature [4]. For example, reconstructing measurements at a higher ambient temperature using calibration data acquired at 0 °C is shown in Fig. 1. Reconstructed photopeak centroids decrease with increasing ambient temperature using voxel-by-voxel gains estimated from a 0 °C calibration. Moreover, energy resolution degrades significantly compared to self-calibrated results. For this work, self-calibrated results are reconstructed by taking a full

* Corresponding author.
E-mail address: jiaweix@umich.edu (J. Xia).

https://doi.org/10.1016/j.nima.2018.10.018
Received 31 July 2018; Accepted 2 October 2018
Available online xxxx
0168-9002/

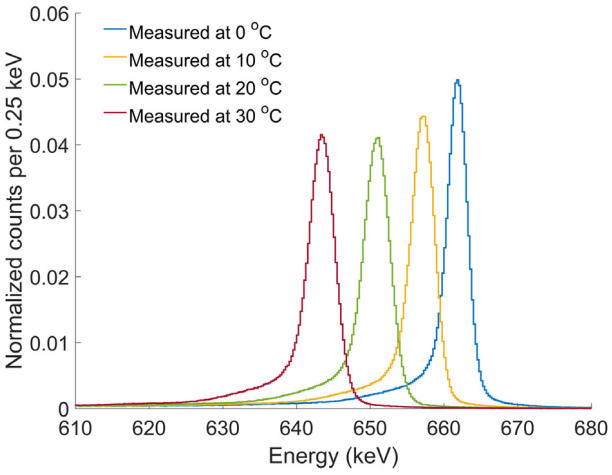

(a) Single-pixel events spectra in photopeak region.

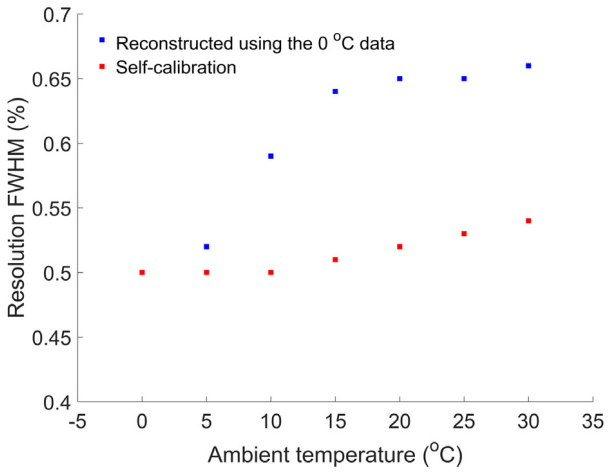

(b) Single-pixel events resolution FWHM at 662 keV

Fig. 1. ^{137}Cs measurements were conducted at different ambient temperatures and reconstructed using a 0°C calibration. Reconstructed peak centroids decrease with increasing ambient temperature. Energy resolution also degrades at higher temperatures. Error bars of resolutions fall within plotted points. The calibration-temperature drift data was acquired using detector 5R-76.

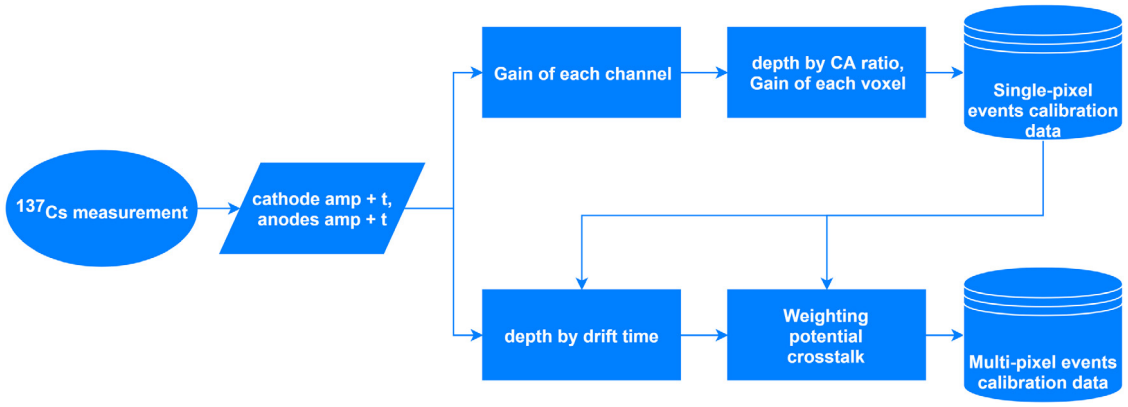

Fig. 2. A simplified flowchart of the calibration process in 3-D CdZnTe detectors.

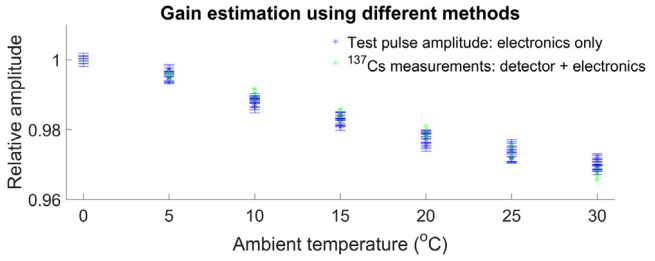

Fig. 3. Relative gain change with temperature, measured using both a ^{137}Cs source and test pulses. Plotted data are from arbitrarily-chosen channels in detector 5R-52. Strong agreement between changes in electronic and total gain are seen.

calibration at a stable ambient temperature, and then applying the calibration parameters to the same measurement. Hence, self-calibrated results benchmark the best achievable performance at each ambient temperature. The change in calibration data due to temperature change is referred to as calibration-temperature drift hereafter.

Temperature regulation is employed in current CdZnTe systems, to eject heat from electronics, to avoid performance degradation from calibration-temperature-drift. However, the regulation of temperature hinders further development of lightweight, hand-held CdZnTe systems. Temperature regulation not only adds to system weight and volume, but also consumes significant power. For example, the Orion UM v1.1 system with nine CdZnTe detectors [1], consumes about 15 W of total power with 7 W used in temperature regulation. If temperature regulation could be avoided, system operation time would increase by over 80% using the same battery. A brute-force approach to discard temperature regulation requires carrying out a full, time-consuming calibration for each temperature. However, this approach is not realistic as calibration time and data storage grow linearly with the increasing temperature-range. An alternative approach, which efficiently corrects for calibration-temperature drift using minimal, additional calibration, is required.

2. Experimental methods

Calibration-temperature drift must be understood in detail to implement an efficient correction. Three Redlen detectors, 5R-18, 5R-52 and 5R-76, were used for analysis. Each detector was connected to a VAD_UM v2.2 application-specific integrated circuit (ASIC) readout system [1] and calibrated at 0, 5, 10, 15, 20, 25 and 30 °C ambient temperatures. The analysis and discussion of this paper is confined to the range of 0 to 30 °C unless otherwise specified. Ambient temperature was controlled in all measurements by placing the detectors and ASICs into an environmental chamber. It should be noted that the true, ambient temperature of the detector is difficult to measure. Instead, in this paper, the detector ambient temperature is the temperature setting of the environmental chamber.

Please cite this article in press as: J. Xia, et al., Efficient temperature corrections for gamma-ray energy reconstruction in 3-D position-sensitive CdZnTe detectors, Nuclear Inst. and Methods in Physics Research, A (2018), https://doi.org/10.1016/j.nima.2018.10.018.

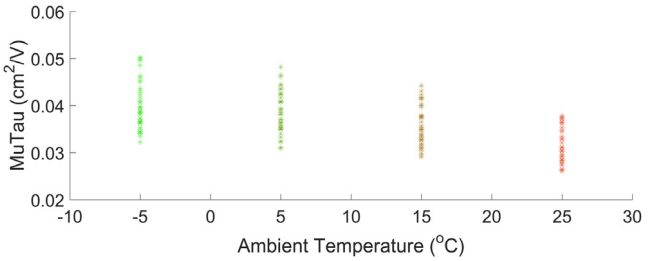

Fig. 4. Measured $\mu_{e,T}\tau_{e,T}$ values for anode channels in detector 5R-76. See [6] for detailed discussion of calculation methods.

For ease of discussion, Fig. 2 presents a simplified calibration process for 3-D CdZnTe detectors. Each 3-D CdZnTe detector is 2 × 2 × 1.5 cm^3 with a common planar cathode and 121 pixelated anode pads. All detectors are operated with the cathode biased at −3000 V. A cathode-side ^{137}Cs flood irradiation calibration measurement was conducted for each detector. Cathode channel amplitude and triggering times alongside all triggered anode channels are measured using digital filters for all events [5].

Events were categorized based on the number of triggered anode pixels. The calibration procedure starts with single-pixel events. First, cathode and anode gains are measured using uncorrected photopeak centroids. Using the measured channel-by-channel gains, the depths of single-pixel interactions can be estimated based on cathode-to-anode signal amplitude ratio (CAR) [7]. The volume under each pixel is artificially subdivided into depth bins, with the space in each bin referred to as a voxel. Since anode channels encode a unique 2-D location, single-pixel events can be placed into 3-D voxels. Voxel-by-voxel, 3-D gains can then be measured using the photopeak centroid of voxel-wise spectra. At least 200 photopeak counts are required in each voxel to avoid overfitting. As a result, calibration measurements must be long enough to record a million photopeak counts. These channel-by-channel gains and voxel-by-voxel gains form the single-pixel events calibration data.

Single-pixel calibrations are also applied to events where multiple anodes trigger. Single-pixel corrections are applied independently to each triggered anode, correcting response non-uniformities from channel-by-channel gain, change of weighting potential field [8] for collecting pixels, and trapping/de-trapping of electrons in the detector. However, there are complicating factors in reconstructing these multi-pixel events. When multiple anode pixels trigger, the depth of each interaction can no longer be calculated using the CAR. Instead, depth is measured by electron drift-time for each interaction. Hole movement is neglected as it does not contribute substantially to signals in 3-D CdZnTe detectors. Due to material and electric field non-uniformities, the relationship between electron drift time and interaction depth in each channel must be mapped using single-pixel events. After the depth of each interaction calculated, single-pixel events calibration data can be applied. In the last step, weighting potential cross-talk ($WPCT$) is measured and corrected. $WPCT$ is the interference between multiple electron clouds as they drift towards the collecting anodes and must be corrected for based on the depth of each interaction, as well as the distance between the interactions. A more detailed discussion of the reconstruction process in 3-D CdZnTe detectors is presented in [7].

3. Analysis and correction for calibration-temperature drift

The effects of temperature change on calibration data was studied in detail to develop an efficient, temperature-based events reconstruction method.

3.1. Channel-by-channel gain vs. temperature

The change in uncorrected, photopeak centroids with ambient temperature is shown in Fig. 3, illustrating that ambient temperature substantially affects channel-by-channel gain. This observed, temperature-dependent gain stems from gain fluctuations in both the detector and readout electronics.

External test pulses were used to isolate electronic gain for each ambient temperature without the detector connected. Relative changes in channel-by-channel gain from ^{137}Cs measurements, which combine electronic and detector gain, and test pulses, which uses electronics alone, are highly correlated as shown in Fig. 3. This implies that the change of electronic gain with temperature is the main cause of channel-by-channel gain change with temperature in ^{137}Cs measurements. Furthermore, channel-by-channel gains are seen to decrease linearly with increasing ambient temperature.

3.2. Voxel-by-voxel gain vs. temperature

Under each pixel the 1.5 cm thickness between the anode and cathode is linearly subdivided into 40 voxels. For simplicity, the direction of the voxelization is called depth (z), ranging from 1 (anode side) to 40 (cathode side). The gain of each voxel under the same pixel can then be represented using Eq. (1).

$$G_T(z) = (g_{e,T})\Delta\varphi(z)exp(-\frac{z}{(\mu_{e,T})(\tau_{e,T})E}) \quad (1)$$

In Eq. (1), $G_T(z)$ represents the gain for gamma-ray events in each depth bin (voxel) along the space under a pixel and is referred to as the gain-depth curve for each anode channel. The subscript, T represents the ambient temperature. The gain-depth curve is the product of three terms: the electronic gain of the anode channel ($g_{e,T}$), change of weighting potential ($\Delta\varphi(z)$) and trapping of electrons ($exp(-z/((\mu_{e,T})(\tau_{e,T})E))$). $\mu_{e,T}\tau_{e,T}$ represents the mobility-lifetime product of electrons in CdZnTe, and E represents the electric field in the detector (assuming it is uniform) [6]. As Section 3.1 discussed, $g_{e,T}$ changes linearly with temperature. $\Delta\varphi(z)$ is a function of z, but not affected by T. $exp(-z/((\mu_{e,T})(\tau_{e,T})E))$ is affected by both z and T , as $\mu_{e,T}\tau_{e,T}$ decreases for increasing T as shown in Fig. 4.

Fig. 5 shows gain-depth curves for a single anode channel of detector 5R-52. As discussed in Section 2, the gain is estimated by measuring the photopeak centroid for spectrum in each voxel. When interactions are close to the anode (z is small), the gain-depth curve increases drastically with increasing z because of the pixelation, known as the small-pixel effect. When interactions are not near the anode, the gain-depth curve changes almost linearly with z because the weighting potential for collecting anode changes much more slowly. The definition of weighting potential and corresponding applications in detector design can be read in [8]. These measured gain-depth curves in 3-D CdZnTe detectors are complex in shape. However, the effect of ambient temperature (T) on gain-depth curves can be approximated using a simpler trend. The $\mu_{e,T}\tau_{e,T}$ values measured in recent, Redlen CdZnTe detectors are usually on the same order of magnitude of 1E-2 cm^2/V [6]. Hence, by Taylor expansion, Eq. (1) can be approximated as:

$$G_T(z) = g_{e,T}\Delta\varphi(z)(1-\frac{z}{\mu_{e,T}\tau_{e,T}E}) = \Delta\varphi(z)(A_T + B_T z) \quad (2)$$

where A_T and B_T are used for easier discussion. They are defined as:

$$A_T = g_{e,T}, \quad (3)$$

$$B_T = -g_{e,T}\frac{z}{\mu_{e,T}\tau_{e,T}E}. \quad (4)$$

Since electron trapping only causes a relatively small deficit in signal amplitude, $|B_T| << |A_T|$. As a result, the relationship between the gain-depth curves for two different temperatures (T and T_0) in the same anode channel can be simplified using Taylor expansion:

$$\frac{G_T(z)}{G_{T_0}(z)} = \frac{A_T + B_T z}{A_{T_0} + B_{T_0} z} \approx [\frac{A_T}{A_{T_0}} + (\frac{B_T}{A_{T_0}} - \frac{A_T B_{T_0}}{A_{T_0}})z]. \quad (5)$$

Please cite this article in press as: J. Xia, et al., Efficient temperature corrections for gamma-ray energy reconstruction in 3-D position-sensitive CdZnTe detectors, Nuclear Inst. and Methods in Physics Research, A (2018), https://doi.org/10.1016/j.nima.2018.10.018.

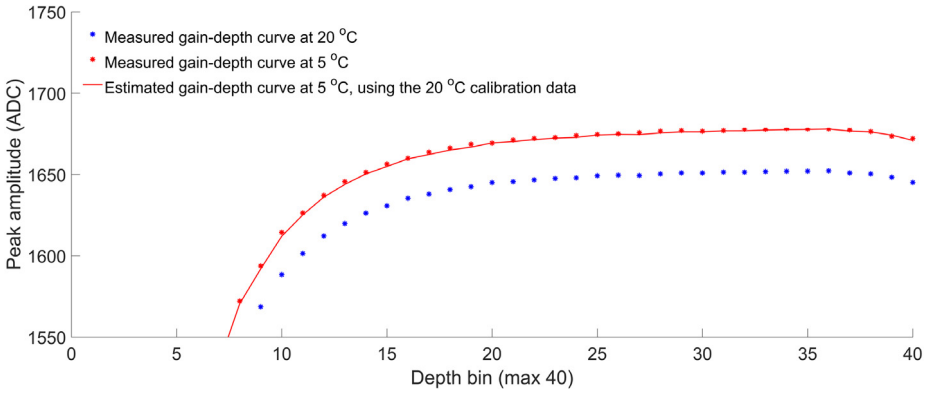

Fig. 5. An example comparing the estimated and measured gain-depth curves at 5 °C for an anode channel in 5R-18. The estimation is based on the linear relationship in Eq. (5), using data from a complete calibration at 20 °C and a short measurement at 5 °C. In this example, the curves slightly decrease when z is very close to 40 (interactions are close to the cathode). This could be caused by various reasons, such as charge collection efficiency degradation or artifacts in the reconstruction. Error bars are negligible and omitted in the figure.

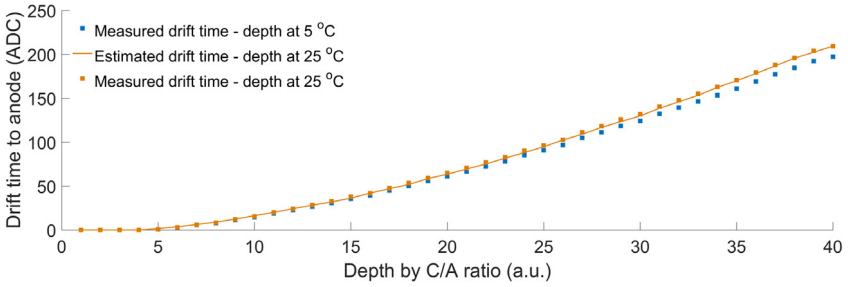

Fig. 6. An example comparing estimated and measured timing-depth curves at 25 °C for one anode channel. The estimate was calculated by linearly re-scaling the timing-depth curve from a complete calibration at 5 °C by a constant, and the constant is the ratio between the maximum drift times for both temperatures.

Eq. (5) implies that although the gain-depth curve for a channel in 3-D CdZnTe detectors is complex, the relative change of the curve between the ambient temperature of T_0 to T can be approximated as a linear function. The linear function's variable is depth, and its intercept and slope are affected by T and T_0. Assume a complete calibration measurement has been taken at ambient temperature T_0, and another, shorter measurement is taken at ambient temperature T. During the short measurement at ambient temperature T the space under each channel can be divided into coarser depth bins. Photopeak centroid amplitudes from interactions in these coarse depth bins can be used in a linear fitting to estimate Eq. (5). This avoids the time consuming collection of 200 photopeak counts per voxel required in full calibrations. As a result, a short measurement at T is enough to estimate the gain-depth curve at T. In this study, a complete calibration measurement using ^{137}Cs usually takes about 2 h. However, with a complete calibration at T_0, 15 min of measurement at other ambient temperatures proved sufficient to estimate the gain-depth curves for all anode channels as shown in Fig. 5.

3.3. Drift time-depth relationship vs. temperature

The relationship between drift time and depth in each channel, called the timing-depth curve, also changes with ambient temperature because the mobility of electrons decreases for higher ambient temperatures. As presented in Fig. 6, at higher temperatures, the electron drift time from the same interaction location to the collecting anode increases. If the timing-depth curves measured at 5 °C are used to reconstruct events measured at 25 °C, the depths of interactions will be systematically overestimated by up to over 1 mm, thus degrading the resolutions of both energy spectrum and Compton imaging. Fortunately, the measurements showed that in each channel, the timing-depth curve for ambient temperature T can be easily estimated by scaling the same curve from a complete calibration at T_0 by a constant value. This value can be easily calculated by measuring the maximum drift times at both temperatures. The maximum drift time corresponds to interactions from the cathode side (z=40), and can be easily measured using only a short measurement.

3.4. Weighting potential crosstalk and nonlinearity vs. temperature

W PCT and nonlinearity corrections are time consuming in CdZnTe detectors. Fortunately, repeated measurements showed that they did not significantly change within the temperature range (0 °C – 30 °C) discussed in this paper.

3.5. Performance of temperature-corrected calibration data

Based on the analyses, a complete calibration at T_0 and a fast measurement at T is sufficient to estimate the complete calibration data at ambient temperature T. This estimation process is referred to as temperature-corrected calibration. ^{137}Cs measurements taken at various ambient temperatures for each detector were reconstructed using both self-calibration and temperature-corrected calibration. The results are compared in Fig. 7. For both single-pixel and all events, the energy-resolution FWHM at 662 keV was only degraded by 0.02 to 0.03% when using temperature-corrected calibration compared to self-calibration. Multi-pixel event results from 5R-18 were omitted as many anode channels showed significant gain variations. The exact reason of this problem is under investigation and is beyond the scope of this paper. However self-calibration requires 2 h of measurement at each temperature while, in contrast, temperature-corrected calibration only requires an additional 15 min for each, additional ambient temperature. Within 0 to 30 °C, with a 5 °C step size, the total calibration time was reduced from 14 to 3.5 h when using temperature-corrected calibration.

Please cite this article in press as: J. Xia, et al., Efficient temperature corrections for gamma-ray energy reconstruction in 3-D position-sensitive CdZnTe detectors, Nuclear Inst. and Methods in Physics Research, A (2018), https://doi.org/10.1016/j.nima.2018.10.018.

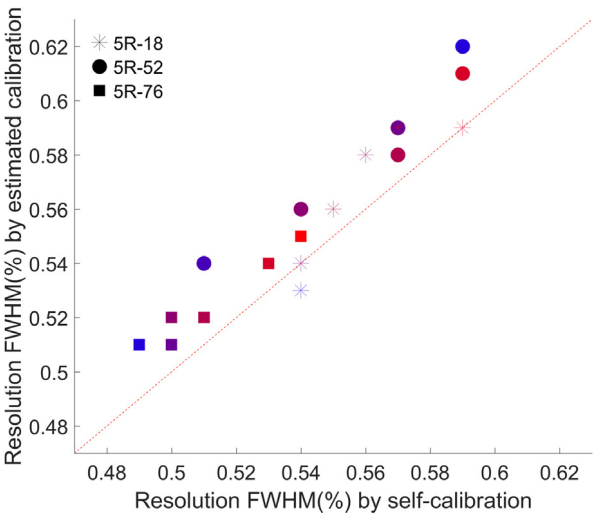

(a) Single-pixel events resolutions FWHM (%).

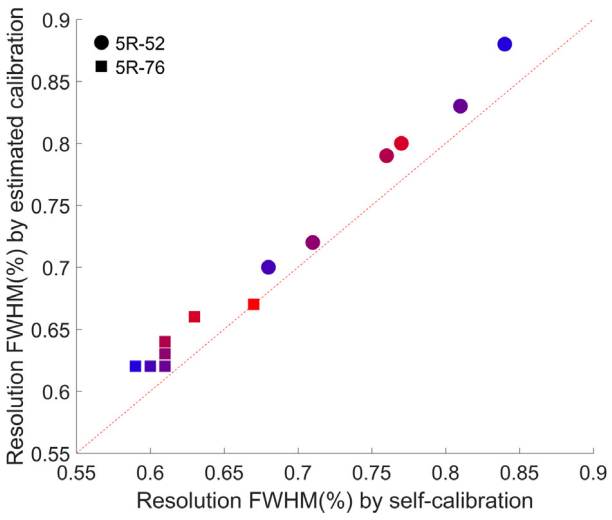

(b) All events resolutions FWHM (%).

Fig. 7. ^{137}Cs measurements were conducted at 0/5/10/15/20/25/30 °C ambient temperatures for each detector and reconstructed using conventional, self-calibration and time-efficient, temperature-corrected calibrations. Different colors represent different ambient temperatures in the measurements. Lower temperature data points are shown in blue while higher temperature data points are shown in red. Dashed lines represent $y = x$, corresponding to no loss in performance relative to the self-calibration benchmark . (For interpretation of the references to color in this figure legend, the reader is referred to the web version of this article.)

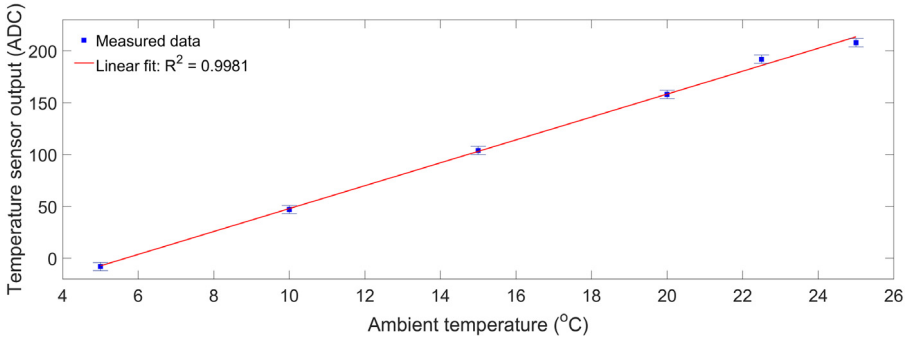

Fig. 8. Comparison between the ASIC temperature sensor and the ambient temperature setting.

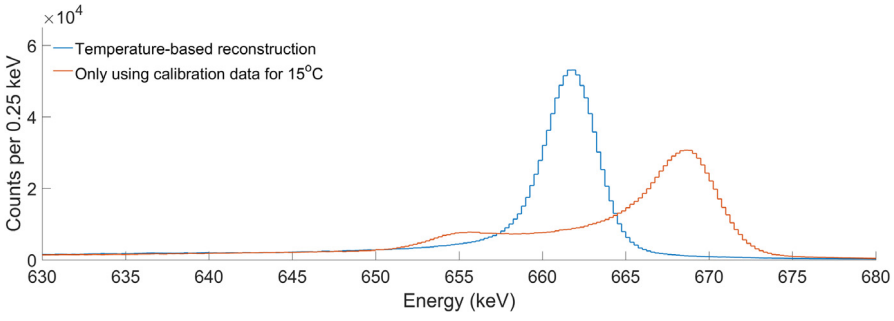

Fig. 9. Single-pixel events spectra, reconstructed by both temperature-based reconstruction and only one calibration dataset for 15 °C. Events were from 5R-52, 25 to 5 °C fast change (Table 1).

4. Events reconstruction based on temperature

Ambient temperature is expected to fluctuate in practical, in-field measurements using hand-held, CdZnTe devices without temperature regulation. A temperature sensor on the VAD_UM v2.2 ASIC was used to measure ASIC and detector temperatures (ASICs are directly coupled to 3-D CdZnTe detectors). As shown in Fig. 8, the ASIC temperature sensor output was linearly related to the ambient temperature of the environmental chamber. However, it should be noted that the measurement was made with the system at thermal equilibrium. In fluctuating ambient temperatures, the ASIC temperature sensor is not guaranteed to truly reflect the detector temperature because of heat transfer and gradient.

Temperature-based events reconstruction can be summarized into two steps. First, a complete calibration and subsequent fast measurements are used to estimate the temperature-corrected calibration data in a temperature range with a certain step size. The calibration data for each temperature is then mapped to a corresponding ASIC sensor output. Linear interpolation is then used in real measurement to estimate the calibration data based on the ASIC sensor output for each event. A

Please cite this article in press as: J. Xia, et al., Efficient temperature corrections for gamma-ray energy reconstruction in 3-D position-sensitive CdZnTe detectors, Nuclear Inst. and Methods in Physics Research, A (2018), https://doi.org/10.1016/j.nima.2018.10.018.

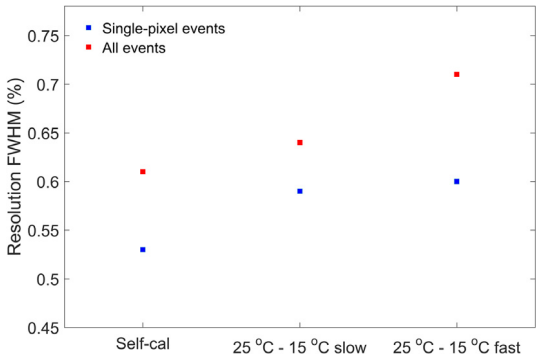

(a) 662 keV events comparison.

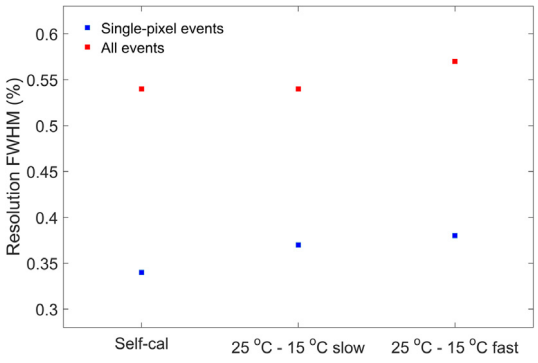

(b) 1332 keV events comparison.

Fig. 10. Temperature-based reconstruction results were compared to self-calibration for gamma ray at 662 and 1332 keV. In the 25 to 15 °C slow change measurement, the ambient temperature setting changed from 25 °C to 15 °C at a constant speed over one hour. In the 25 to 15 °C fast change measurement, the ambient temperature setting changed from 25 °C to 15 °C instantaneously during the beginning of the one-hour measurement. Self-calibration results are also shown for comparison.

Table 1
Energy resolution FWHM at 662 keV for different measurements and reconstructions: 25 °C measurements are reconstructed using self-calibration while transient measurements were reconstructed using temperature-corrected calibrations. Multi-pixel events results from 5R-18 are omitted due to gain variation problems.

Detector	Event types	25 °C equilibrium [a]	25 to 5 °C fast change [b]
5R-18	Single-pixel	0.55%	0.62%
5R-52	Single-pixel	0.58%	0.61%
5R-52	All events	0.68%	0.73%
5R-76	Single-pixel	0.53%	0.61%
5R-76	All events	0.63%	0.71%

[a]Reconstructed using self-calibration.
[b]Reconstructed using temperature-corrected calibration.

practical performance evaluation of the temperature-based reconstruction method was made by quickly changing ambient air temperature during a measurement. To start, each detector was at equilibrium with the environmental chamber set to 25 °C. The environmental chamber was then set to 5 °C and an one-hour, ^{137}Cs flood irradiation from the detector cathode side was started. One hour measurement duration was chosen to ensure that the detector temperature reached the new equilibrium. Drierite was used in the environmental chamber to mitigate condensation. In the field, a hand-held CdZnTe device might experience a similar change in ambient temperature when the user enters or exits a building.

As Table 1 shows, the energy resolution of temperature-corrected measurements during the transients were worse than steady-state results in Fig. 7. This degradation was expected, since the ASIC sensor will not always truly reflect the temperature on the detector when ambient temperature changes rapidly. Still, the most significant degradation was within 0.1%. Fig. 9 shows the single-pixel events spectrum peak shape using the temperature-based reconstruction method during the transient. In comparison, it also presents the peak shape when only one data is using during the temperature transient. It should be noted than when only one calibration dataset is used, the energy resolution of the resulting spectrum was degraded to 0.82%. In addition, the complex peak shape cause by gain-drift make it difficult for peak fitting algorithms to distinguish gamma-ray lines that are close in energy.

To further prove that heat transfer during temperature variation can degrade energy resolution, repeated measurements were conducted using detector 5R-76. In each measurement, a ^{137}Cs source and a ^{60}Co source were used to flood irradiate the detector from the cathode side. For different measurements, the ambient temperature settings changed at different paces from 25 °C to 15 °C as shown in Fig. 10. When the temperature changed at a slow, constant speed, reconstructions using temperature-based method showed less degradation when compared to measurements with a fast transient.

5. Conclusion

Three Redlen CdZnTe detectors were tested at different ambient temperatures ranging from 0 to 30 °C. Analysis shows that changes in electronic gain and electron mobility-lifetime product are the main causes of calibration-temperature drift. A method was then proposed that used one full calibration and several fast measurements at different ambient temperatures to efficiently estimate corrections across a wide range of ambient temperatures. The estimated datasets showed almost identical performance to calibrations generated by a long measurement for each temperature. Measurements were also conducted with the ambient temperature changing. Based on the ASIC temperature sensor, a linear interpolation was used to generate calibrations on an event-by-event basis. Results show that compared to self-calibrated results at a stable ambient temperatures, the degradation in all events energy resolution is at most 0.1% when the ambient temperature changed very quickly without temperature regulation. Hence, it is possible to reduce the weight and size of hand-held, 3-D CdZnTe devices at a small cost of energy resolution ($< 0.1\%$) and calibration time.

Acknowledgments

This work was supported in part by the U.S. Department of Defense, Defense Threat Reduction Agency under Award No. HDTRA1-15-C-0049. Any opinions, findings, and conclusions or recommendations are those of the authors and do not necessarily reflect the views of the Defense Threat Reduction Agency.

The authors would also like to thank David Goodman for constructive criticism of the manuscript.

References

[1] Y. Zhu, M. Streicher, J. Xia, Z. He, Energy resolution improvement and high-energy photon detection in cdznte spectrometers with second generation digital electronics and reduced preamplifier trace length, submitted.
[2] S. Brown, Time-Encoded Thermal Neutron Imaging using Large-Volume Pixelated CdZnTe Detectors (Ph.D. thesis), University of Michigan, 2017.
[3] J. Chu, Advanced Imaging Algorithms with Position-Sensitive Gamma-Ray Detectors (Ph.D. thesis), University of Michigan, 2018.
[4] J. Mann, Improving Cadmium Zinc Telluride Spectrometer Performance and Capabilities (Ph.D. thesis), University of Michigan, 2016.
[5] Y. Zhu, Digital Signal Processing Methods for Pixelated 3-D Position Sensitive Room-Temperature Semiconductor Detectors (Ph.D. thesis), University of Michigan, 2012.
[6] J. Xia, M. Streicher, Y. Zhu, Z. He, Measurement of electron mobility-lifetime product in 3d position-sensitive cdznte detectors using the vad_umv2.2 digital readout system, http://dx.doi.org/10.1109/TNS.2018.2876021.
[7] F. Zhang, Events Reconstruction in 3-D Position Sensitive CdZnTe Gamma-Ray Spectrometers (Ph.D. thesis), University of Michigan, 2005.
[8] Z. He, Review of the shockleyramo theorem and its application in semiconductor gamma-ray detectors, Nucl. Instrum. Methods Phys. Res. A 463 (1–2) (2001) 250–267.

Please cite this article in press as: J. Xia, et al., Efficient temperature corrections for gamma-ray energy reconstruction in 3-D position-sensitive CdZnTe detectors, Nuclear Inst. and Methods in Physics Research, A (2018), https://doi.org/10.1016/j.nima.2018.10.018.